Scientific Research Publishing

Atmospheric and Climate Sciences, 2026, 16(1), 71-82
https://www.scirp.org/journal/acs
ISSN Online: 2160-0422
ISSN Print: 2160-0414

Time Lag and Amplitude Differences between Correlated Variables in Global Temperature Changes

Masaharu Nishioka

Chicago, IL, USA
Email: m.nishioka@sbcglobal.net

How to cite this paper: Nishioka, M. (2026) Time Lag and Amplitude Differences between Correlated Variables in Global Temperature Changes. *Atmospheric and Climate Sciences*, **16**, 71-82.
https://doi.org/10.4236/acs.2026.161005

Received: October 29, 2025
Accepted: December 2, 2025
Published: December 5, 2025

Abstract

Temperature changes were investigated via Fourier analysis for the entire globe, the 48 states, and the Japanese archipelago. A comparison of power spectra revealed that the amplitude of temperature changes in the Japanese archipelago was greater than that for the entire globe or the 48 states. The amplitude was particularly amplified during El Niño events. Temperature changes were observed with regular phase cycles. A similar Fourier analysis was performed on the correlation between the global temperature and the rate of increase in the CO_2 concentration reported in previous studies. The rate of increase in the CO_2 concentration was also confirmed to change with a regular phase cycle. Furthermore, a phase shift was confirmed between the two. Previous studies have shown that there is a time lag between the two, with temperature changes preceding the rate of increase in the CO_2 concentration. This result contradicts the IPCC's theory that global warming is due to increased anthropogenic CO_2 concentrations. Temperature changes in specific regions can deviate significantly from global temperature changes. This deviation is even greater during El Niño events. Therefore, when considering global warming based on temperature changes in specific regions, care must be taken not to make excessive inferences.

Keywords

Global Warming, Cross-Correlation, Time Lag, El Niño, Fourier Analysis, Power Spectra, CO_2 Concentration

1. Introduction

El Niño events are characterized by warmer-than-average sea surface temperatures in the central and eastern tropical Pacific Ocean. This phenomenon disrupts

atmospheric circulation and leads to a chain of climate impacts worldwide [1]-[3]. For example, in Peru and Ecuador, heavy rainfall and floods can occur. Conversely, the Amazon basin and northeastern Brazil often experience drought and forest fires. The southern U.S. tends to have wetter and cooler-than-average winters, whereas the northern U.S. and Canada experience milder winters. Southeast Asia, India, and Australia typically face droughts, which can lead to severe agricultural issues and an increased risk of wildfires. Eastern Africa, particularly Kenya, often experiences above-average rainfall and floods, whereas southern Africa experiences drier conditions. For tropical cyclones, El Niño events suppress hurricane activity in the Atlantic Ocean but increase it in the Pacific Ocean.

When we look at temperature changes, the global average temperature generally increases during El Niño events, whereas the global average temperature decreases during La Niña events. However, owing to the influence of ocean currents and winds on the Earth's surface, the temperature in a particular region may not necessarily be the same as the average temperature change. As summarized above, the temperature in a specific area may be significantly higher or lower than the average temperature change.

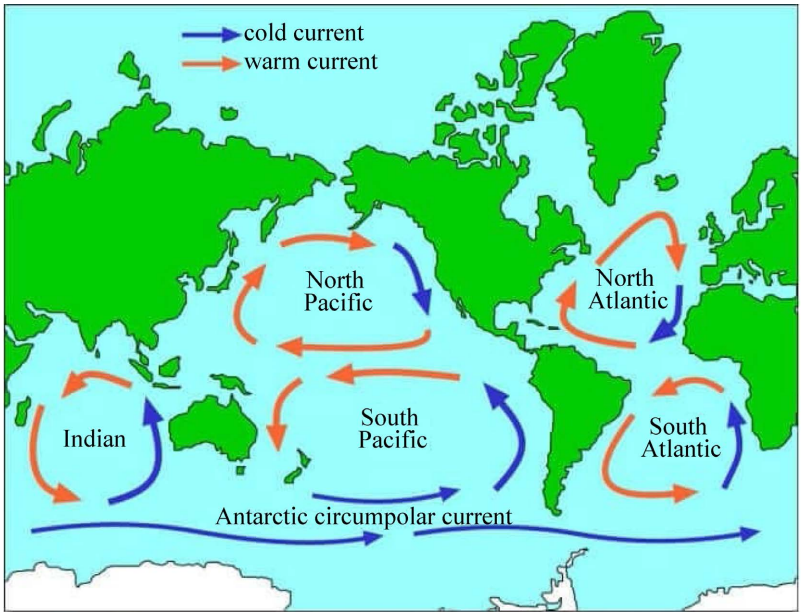

Figure 1. This map broadly shows the formation of different gyres in the ocean [5].

As described in a previous paper [4], the Niño 3.4 region, which is used to monitor the Oceanic Niño Index (ONI), is located near the equator, and the ocean currents flowing through this region head westward. At the western end of the Pacific Ocean, they subsequently turn northward in the Northern Hemisphere, as shown in **Figure 1** [5]. The warm current flowing east of the Japanese Islands is called the "*Kuroshio*" Current (**Figure 2**) [6]. During El Niño events, the Kuroshio Current may cause an increase in temperature near the Japanese Islands. During the 2003-2005 El Niño period, the Japanese Island experienced a temperature in-

crease that was greater than the change in the global average temperature. In Japan, days with a maximum daily temperature of 35˚C or higher are called "extremely hot days," and warnings are issued to prevent heatstroke. The number of such extremely hot days increases during the El Niño period, as shown by the statistics for Tokyo in **Figure 3** [7]. "*Honshu*", the largest of Japan's four main islands, is located between 33˚N and 42˚N. While this island is in the temperate zone, there are a considerable number of days during the El Niño period when temperatures are higher than those in the tropical zone.

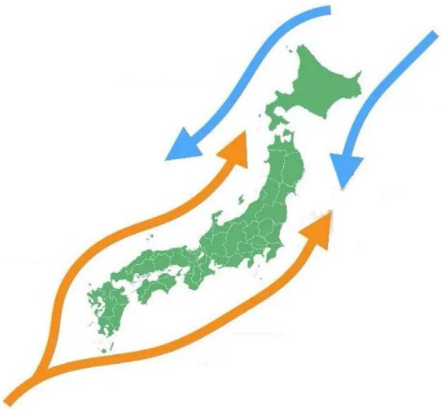

Figure 2. Ocean currents surround the Japanese archipelago [6].

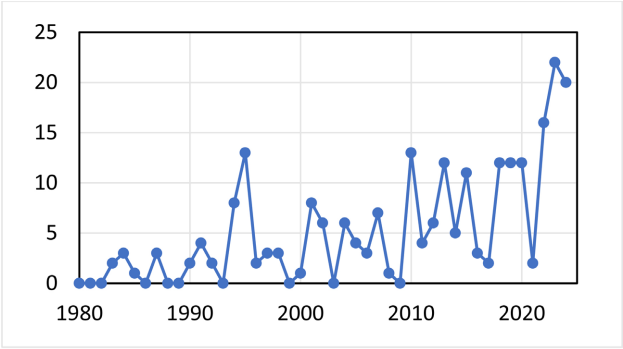

Figure 3. Change in extremely hot days (≥35˚C) in Tokyo [7].

As briefly mentioned above, there may be a correlation between temperature changes in a specific small area and temperature changes in a wider area. However, even if a correlation exists, the magnitude of the change may vary. Other physical variables affect weather in addition to temperature, such as rainfall, the frequency of typhoons, the direction of ocean currents, cloud movement, and large global wind changes. Furthermore, changes in CO_2 concentration, which have attracted attention in recent years, may be a critical weather factor.

For these reasons, the purpose of this study is to present a general analysis of changes in the physical quantities of meteorological factors that may be correlated at two points. Therefore, this study focuses on temperature changes in the Japanese archipelago as a specific, small region compared with the global average warming

trend. Furthermore, the same analysis method is applied to the correlation between global temperature changes and CO_2 concentration changes. The correlation between global temperature changes and CO_2 concentration changes is then examined in comparison with the two methods used in the previous analysis [8].

2. Global Data

Since 1979, the University of Alabama in Huntsville (UAH) has updated global temperature datasets that represent the piecing together of temperature data from a total of fifteen instruments flying on different satellites. Further details are available [9]. Temperatures here were obtained from the datasets, and the 13-month average of lower troposphere anomaly values was used, where the temperatures were averaged over the 6 months before and after each specific month.

The annual mean growth rate of CO_2 in a given year is the difference in concentration between the end of December and the start of January of that year reported by the National Oceanic and Atmospheric Administration (NOAA). Further details are available on their website [10]. The "annual mean growth rate" reported by NOAA is used in many other cases, and the NOAA website provides a graph of the "annual mean growth rate". In this paper, we also analyze the "monthly growth rates" available from NOAA. Because of the seasonal changes in CO_2 concentrations, the annual means and the monthly data are used.

Monthly average temperature data in Japan were obtained from 15 locations selected from meteorological observation stations that have been conducting observations since 1898 by the Japan Meteorological Agency, with little impact from urbanization and no bias toward specific regions. For each location, the deviation of the monthly average temperature (observed monthly average temperature minus the 30-year average from 1991 to 2020) is calculated. The annual average values from the Japan Meteorological Agency were also cited for seawater temperatures near Japan [11].

In general, the correlation coefficient r between variables x and y can be defined as follows:

$$r = \frac{\frac{1}{n}\sum_{i=1}^{n}(xi-\overline{x})(yi-\overline{y})}{\sqrt{\frac{1}{n}\sum_{i=1}^{n}(xi-\overline{x})^2}\sqrt{\frac{1}{n}\sum_{i=1}^{n}(yi-\overline{y})^2}} \quad (1)$$

For convenience, r can be easily calculated via built-in functions in Microsoft Excel®. This calculated r is used to show correlations between two variables throughout this paper.

Fourier analysis of physical parameters over time provides the power spectra. For convenience, the power spectra can be easily calculated via built-in functions in Microsoft Excel®. In this paper, we compare power spectra obtained via Fourier transforms. The data obtained from meteorological observations are, by definition, real numbers. The Fourier transform of a real signal has conjugate symmetry, and the resulting power spectrum is bilaterally symmetric. Because of the compu-

tational efficiency of an algorithm for quickly calculating the discrete Fourier transform (DFT), it is common to set the number of data points to a power of 2. In this study, 512 data points are mostly set.

3. Results and Discussion

The amplitude of temperature change in the Japanese archipelago is compared to that in the global temperature or in the 48 states of the USA in Figure 4(a) or Figure 4(b), respectively. The global temperature and temperature in the 48 states of the USA are measured through satellites, whereas the temperature in the Japanese archipelago is observed on the ground. However, the amplitude of temperature change in the Japanese archipelago is obviously larger than that globally or in the 48 states of the USA. Additionally, the amplitude of the temperature change in the 48 states of the United States is greater than that of the global temperature. Temperature changes are particularly amplified during ENSO events in 1990, 1994, 2003, 2019, and 2023. While their frequency can be quite irregular, El Niño and La Niña events occur on average every 2 - 7 years [12].

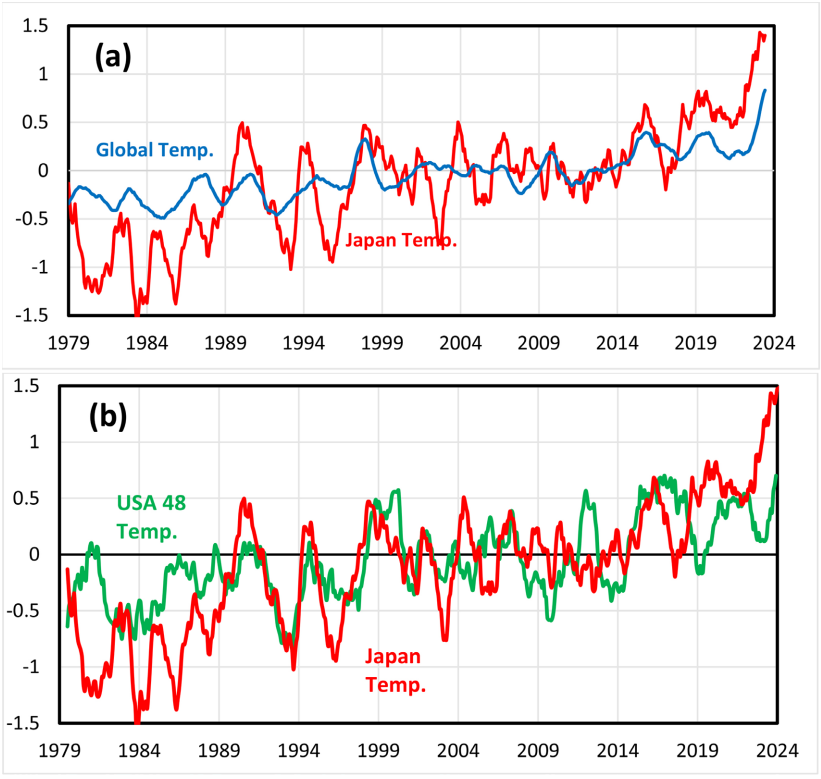

Figure 4. (a) Comparison of the amplitude of temperature changes in the Japanese archipelago and in the global temperature; (b) Comparison of the amplitude of temperature changes in the Japanese archipelago and in the 48 states of the USA.

Figures 5(a) and Figure 5(b) show power spectra obtained via Fourier transforms for temperatures in the Japanese archipelago, globally, or in the 48 states of the USA. As seen in the temperature amplitude changes in Figures 4(a) and Fig-

ure 4(b), the amplitude fluctuations of the power spectrum are very small for the entire Earth in Figure 5(a). On the other hand, significant amplitude changes are observed for temperatures in both the Japanese archipelago and the 48 states of the United States. Furthermore, a regular phase frequency of the temperature changes is observed.

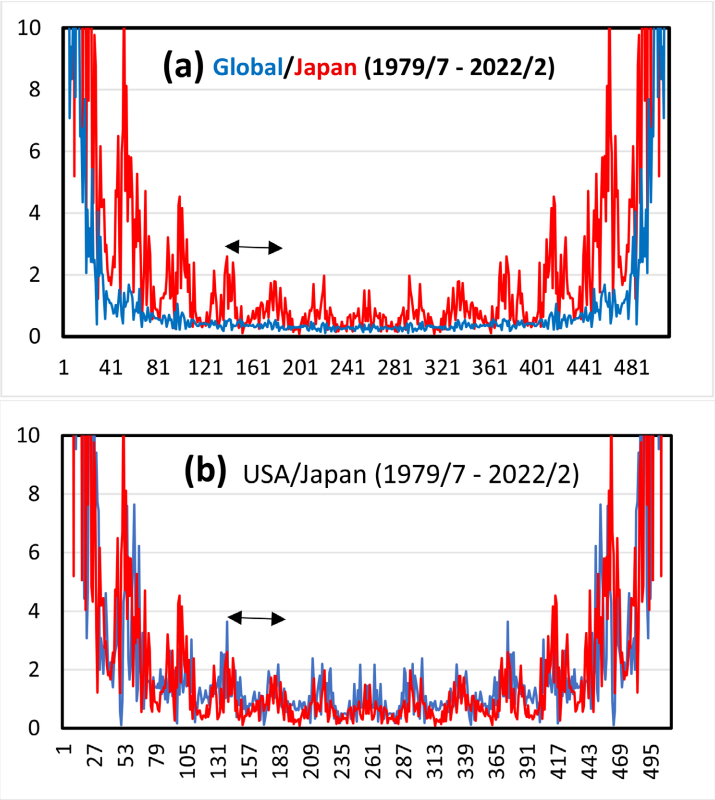

Figure 5. (a) Comparison of power spectral density obtained via Fourier transforms for temperatures in the Japanese archipelago and globally; (b) Comparison of power spectral density obtained via Fourier transforms for temperatures in the Japanese archipelago and in the 48 states of the USA (The horizontal axis represents the number of data points from the start of the analysis. The number of data points is the same as the number of months).

Global temperature anomalies and CO_2 annual growth rates are correlated over 40 years, as reported in our recent paper [8]. The 12-month average CO_2 annual growth rates are reported by NOAA [10]. The latest correlation between July 1979 and December 2023 is shown in Figure 6(a). Its correlation coefficient r is 0.744, and the correlation is relatively good [8].

Figure 6(b) shows the power spectra of global temperature anomalies and CO_2 annual growth rates shown in Figure 6(a). Regular frequency patterns are observed for both global temperature anomalies and CO_2 annual growth rates. Additionally, a phase shift between these frequencies is observed by comparing the double-headed arrows on the two power spectra in Figure 6(b). In addition, no such phase shift is observed between the two power spectra of temperatures over the 48 states and the Japanese archipelago in Figure 5(b).

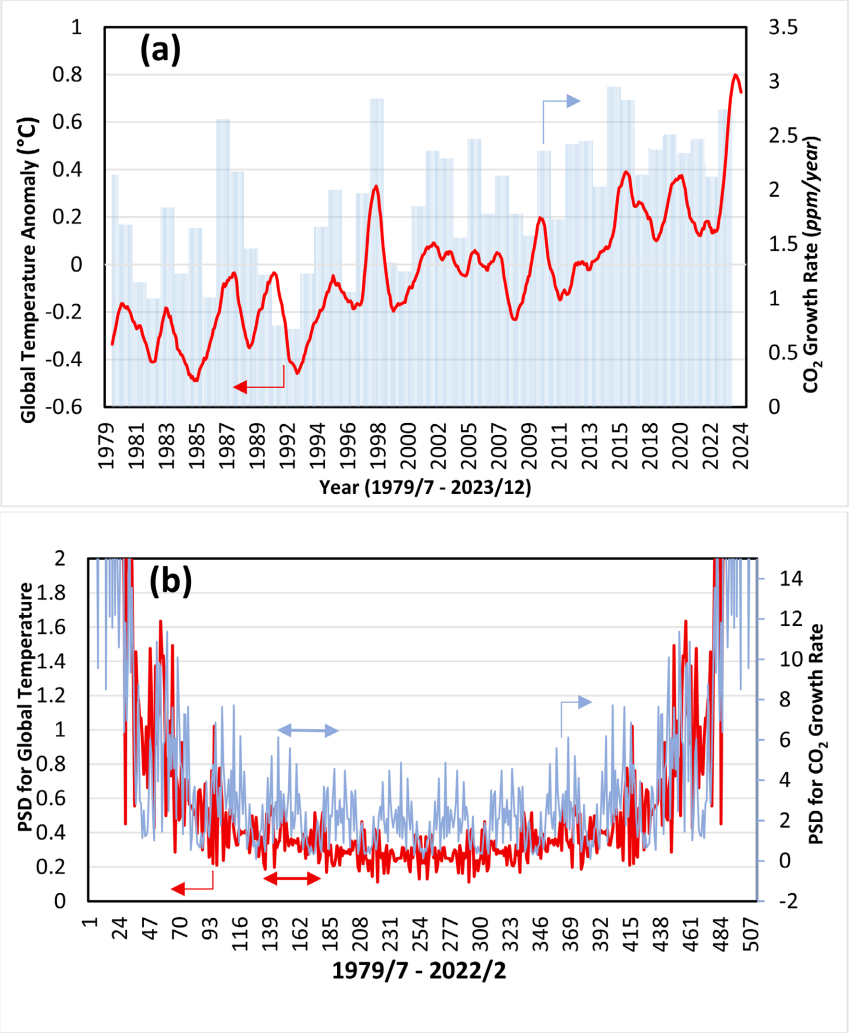

Figure 6. (a) Correlation of the global temperature anomaly (red line, scale: left axis, ˚C) and 12-month average annual CO_2 growth rates (blue bar, scale: right axis, ppm/year); (b) Comparison of power spectral density (PSD) obtained via Fourier transforms for the global temperature anomaly and 12-month average annual CO_2 growth rates (The horizontal axis represents the number of data points from the start of the analysis. The number of data points is the same as the number of months).

The power spectrum represents the strength of the vibrational components of a signal at each frequency. However, because it does not include information about the phase (time lag), it is impossible to determine the direction of the time lag. Quantitative analysis of the time lag requires the use of a cross-correlation function or cross-spectrum (cross-spectral density). Automating calculations via the cross-correlation function or cross-spectrum requires specialized software. The cross-correlation function can be calculated relatively easily via built-in functions in Microsoft Excel®. In a previous paper, we used the cross-correlation function to examine the time lag between two variables. On the basis of this information, we can attempt to interpret the power spectrum in Figure 6(b).

The time lag between changes in global temperature and CO_2 concentration

was investigated via two different methodologies described in previous papers [4] [8]. Murry Salby analyzed the change in temperature (ΔT) and the change rate of the CO_2 concentration (rCO_2) and suggested that the change rate of the CO_2 concentration ($drCO_2/dt$) can be expressed as Equation (2) [13] [14].

$$d(rCO_2)/dt = \gamma\Delta T \quad (2)$$

where γ is a constant. In the paper [8], time lags for selected ENSO events were analyzed. The CO_2 concentration shows a regular pattern of minimum values in August and maximum values in May each year. Therefore, for each year, we considered the change in CO_2 over the course of a year, starting from September, as increased CO_2 (ΔCO_2). The temperature change (ΔT) is considered to be the amount of change from the reference value when the CO_2 increase (ΔCO_2) is considered. Temperatures rise in response to the occurrence of El Niño. CO_2 concentrations also increase in response to temperature increases. The deviations in ΔCO_2 and ΔT between the El Niño period and the period before El Niño were considered. The correlation coefficient r is maximized by shifting ΔT by five months. This means that the CO_2 concentration is determined by temperature changes, but with a 5-month time lag. The results prove Equation (2).

Since the 13-month average of temperature change and the annual average of the rate of CO_2 increase are used in **Figure 6(a)**, a time lag less than 12 months between the two variables cannot be effectively analyzed. Another paper [4] compared global temperature anomalies and CO_2 *monthly* growth rates instead of CO_2 *annual* growth rates between 1980 and 2023. The correlation coefficient between the two is 0.664. The CO_2 growth rates lag behind the global temperatures. Therefore, the correlation coefficient between the CO_2 growth rates and global temperatures was investigated by changing the lag time (in months). The value at which the correlation coefficient r is maximized indicates that the CO_2 growth rate changes with a lag of approximately four months compared with the global temperature.

The peak of the power spectrum can be said to represent the dominant frequency component in the time series data. The frequency at which the peak appears can be interpreted as the frequency that most strongly characterizes the rhythm and fluctuation pattern of the entire time series signal. Based on this interpretation, the following can be considered: Regular phase patterns are observed in both the global temperature anomaly and the annual CO_2 increase rate. Furthermore, a phase shift is observed between the two. The difference between the global temperature anomalies and CO_2 annual growth rates in the power spectra of **Figure 6(b)** may be interpreted as a time lag between the two, as referred to the results from previous papers [4] [8]. The previous results also revealed that global temperature anomalies and CO_2 annual growth rates and that global temperature anomalies are ahead of CO_2 annual growth rates. All the results obtained via the three different methodologies confirmed the time lag between changes in the global temperature and CO_2 concentration, and in particular, changes in the global temperature preceded changes in the CO_2 concentration, as confirmed via the correlation coefficient r.

An increase in global CO_2 emissions and a subsequent increase in global temperature proposed by the Intergovernmental Panel on Climate Change (IPCC) were not observed, but an increase in global temperature, an increase in soil respiration, and a subsequent increase in global CO_2 emissions were noted [8]. This natural process can be clearly detected during periods of increasing temperature, specifically during El Niño events. The results cast strong doubts that anthropogenic CO_2 is the cause of global warming. This paper analyzes global mean temperatures reported by UAH using satellites since 1979. The observation period is very short compared to the global time scale, and the discussion is based on the results of the analysis within this time limit.

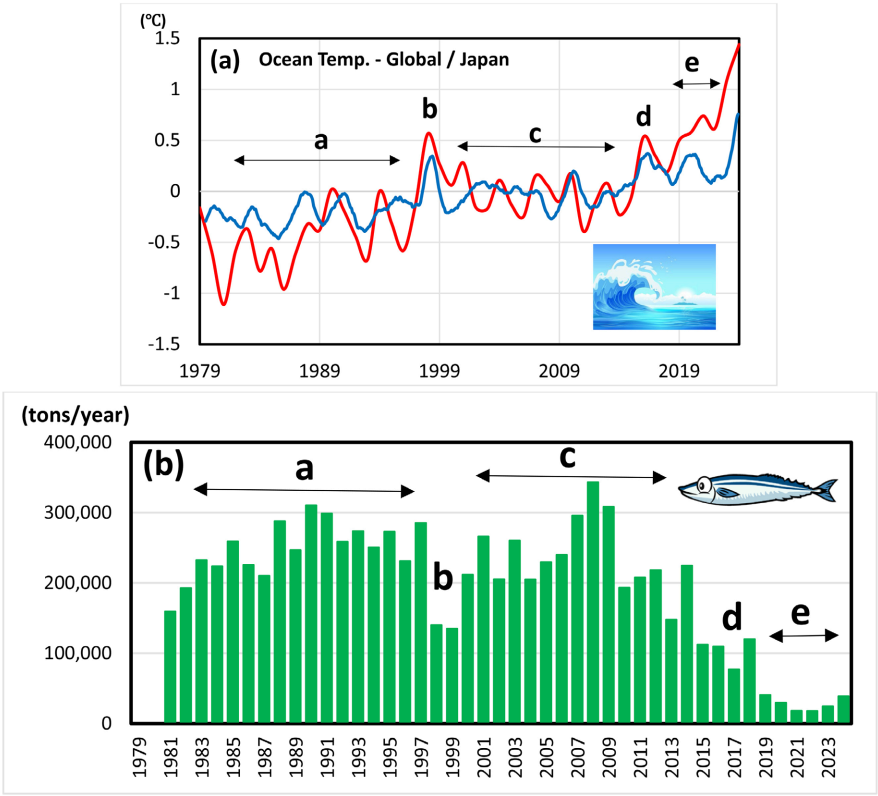

Figure 7. (a) Comparison of sea water temperatures around the world and near Japan; (b) Changes in saury catch volume [15].

Above, we used the Japanese archipelago as an example to demonstrate that while there is a correlation between the average temperature in a specific region and the global average temperature, the temperature in that specific region can be significantly amplified compared with the global average temperature. This correlation is thought to be due primarily to the influence of the ocean. Below, we use analytical results to demonstrate the correlation between the amplification of temperature changes in the Japanese archipelago and seawater temperature. In fact, global temperature changes correspond to seawater temperature changes, with a correlation coefficient of r = 0.99 [4]. **Figure 7(a)** compares the global and Japa-

nese seawater temperatures. Here, the global seawater temperature is the monthly 13-month average, whereas the seawater temperature in Japanese seawater is the annual average. Compared with **Figure 4(a)**, the temperature in the Japanese archipelago corresponds to the seawater temperature in Japanese seawater. **Figure 7(b)** shows the change in saury catch (tons) in Japan [15]. Points b, d, and e indicate El Niño periods. During these El Niño periods, seawater temperatures were also higher than those in other periods. Interestingly, as shown in **Figure 7(b)**, fluctuations in saury catch correspond to changes in seawater temperature. Points b, d, and e in the figure indicate high temperatures during El Niño periods, when saury catches were low. The decline in saury catches in Japanese seawater has been linked to fluctuations in seawater temperature [16]. Saury prefers water temperatures between 15˚C and 20˚C, and their typical autumn migration pattern involves moving south along the Japanese coast. However, with the recent rise in seawater temperature, saury schools are increasingly migrating offshore, away from the Japanese coast.

4. Conclusions

The results obtained in this study can be summarized as follows:

1) The amplitude of temperature change in the Japanese archipelago is larger than that globally or in the 48 states of the USA.

2) The amplitude of temperature change is particularly amplified during ENSO events.

3) A comparison of the power spectrum of temperature change over time via Fourier analysis revealed a regular phase cycle of temperature change in both the Japanese archipelago and the 48 states of the United States.

4) As reported in previous research [4], there is a correlation between the global temperature and the CO_2 growth rate.

5) A similar Fourier analysis was performed on global temperature changes and CO_2 concentration growth rates. Both change with a regular phase cycle and are out of phase with each other. Temperature changes increase the CO_2 concentration by approximately six months.

6) The global temperature change corresponded to the change in seawater temperature, with $r = 0.99$ [4]. Temperatures in the Japanese archipelago also correspond to seawater temperatures near Japan.

7) Interestingly, changes in seawater temperature near Japan correspond to changes in saury catches.

8) Temperature changes in a specific region can deviate significantly from global temperature changes. This deviation is greater during ENSO events. Therefore, when considering global warming based on specific temperature changes, it is important to be careful not to make large inferences.

Conflicts of Interest

The author declares no conflicts of interest regarding the publication of this paper.

References

[1] NOAA: El Niño Suppresses Hurricane Activity in the Atlantic Ocean But Increases It in the Pacific Ocean. https://www.climate.gov/news-features/understanding-climate/el-nino-and-la-nina-frequently-asked-questions

[2] WMO: NOAA. https://wmo.int/news/media-centre/el-nino-weakens-impacts-continue

[3] NASA: El Niño. https://science.nasa.gov/earth/explore/el-nino/

[4] Nishioka, M. (2025) Time Lag in Changes in Global Temperature and Co_2 Concentration Following Changes in the Oceanic Niño Index. *Atmospheric and Climate Sciences*, **15**, 668-680. https://doi.org/10.4236/acs.2025.153033

[5] UPSC Ocean Currents. https://lotusarise.com/ocean-currents-upsc/

[6] Modified. https://katekyo.mynavi.jp/juken/5308

[7] Japan Meteorological Agency: Extremely Hot Days. https://www.data.jma.go.jp/cpdinfo/himr/himr_tmaxGE35.html

[8] Nishioka, M. (2024) Cross-Correlation between Global Temperature and Atmospheric CO_2 with a Temperature-Leading Time Lag. *Atmospheric and Climate Sciences*, **14**, 484-494. https://doi.org/10.4236/acs.2024.144029

[9] Latest Global Temps. https://www.drroyspencer.com/latest-global-temperatures/

[10] Lan, X., Tans, P., *et al.* (2023) Trends in Globally Averaged CO_2. NOAA Global Monitoring Laboratory Measurements. Version 2023-08. https://doi.org/10.15138/9N0H-ZH07

[11] Japan Meteorological Agency: The Deviation of the Monthly Average Temperature. https://www.data.jma.go.jp/cpdinfo/temp/list/mon_jpn.html

[12] NOAA: ENSO Some Basics. https://psl.noaa.gov/enso/enso_101.html

[13] Salby, M. (2016) Atmospheric Carbon. Video Presentation, University College London. https://www.youtube.com/watch?v=3q-M_uYkpT0

[14] Salby, M. (2018) What Is truly Behind the Increase of Atmospheric CO_2? Video Presentation, Helmut-Schmidt-University Hamburg. https://www.youtube.com/watch?v=rohF6K2avtY

[15] The National Sanma Stick Fishing Cooperative: Catch Volume Data. https://www.samma.jp/tokei/catch_year.html

[16] Japan Meteorological Agency: Sea Temperature Data. https://www.data.jma.go.jp/kaiyou/data/shindan/a_1/japan_warm/japan_warm.html

Abbreviations

ONI	Oceanic Niño Index
ENSO	El Niño-Southern Oscillation
IPCC	Intergovernmental Panel on Climate Change (the United Nations body)
NOAA	National Oceanic and Atmospheric Administration
UAH	University of Alabama in Huntsville
r	Correlation Coefficient